Quaternary Research (2024), **117**, 30–42
doi:10.1017/qua.2023.27

Research Article

Changes in the lake-grassland ecosystem revealed by multiple proxies in a sediment core from Ganggeng Nur Lake, northern China

Liang Li[a,b], Zhi Zhang[c], Zhenyu Ni[a], Weiwei Sun[a], Xianqiang Meng[a], Enlou Zhang[a], Guangwei Zhu[a], Yunlin Zhang[a] and Boqiang Qin[a]

[a]State Key Laboratory of Lake Science and Environment, Nanjing Institute of Geography and Limnology, Chinese Academy of Sciences, 73 East Beijing Road, Nanjing 210008, China; [b]University of Chinese Academy of Sciences, Beijing 100049, China and [c]School of Ecology and Environment, YuZhang Normal University, 1999 Meiling Avenue, Nanchang 330022, China

Abstract

As the main global terrestrial ecosystem component, grasslands are extremely sensitive to global climate change. With increasing human activities over the last century, grassland ecosystems have been degraded to different degrees. However, the evolution of lake-grassland ecosystems in recent centuries remains unclear due to the dearth of high-resolution records. Here, we present high-resolution lacustrine sediment grain size, pollen (*Artemisia*, *Myriophyllum*), *Pediastrum*, and n-alkane records from Ganggeng Nur Lake to investigate vegetation, lake evolution, and human effects in semiarid northern China. Four stages were identified from the last ca. 150 years: (1) the natural evolution stage (AD 1870–1945), in which there was a wet climate around Ganggeng Nur and the lake level rose from increased runoff; (2) the human disturbance stage (AD 1945–1967), in which the regional climate got drier and human activities began having a detectable effect on the grassland ecosystem; (3) the human transformation stage (AD 1967–2005), in which a completely arid climate coupled with the implementation of a series of land reclamation policies resulted in a large reduction in grassland areas, extensive soil erosion, exacerbated climate change, and shrinking lake areas; and (4) the posttreatment stage (AD 2005–2018), in which soil erosion was alleviated by policy implementation and a favorable humid climate.

Keywords: Lacustrine sediment, Sediment grain size, Pollen, N-alkanes, Lake-grassland ecosystem, Human activity

(Received 5 September 2022; accepted 10 May 2023)

INTRODUCTION

As an important component of freshwater resources, lakes are crucial for the reproduction and biodiversity of various organisms (Tao et al., 2015; Feng et al., 2016). This is especially true for lakes of Inner Mongolia—a typical arid and semiarid region (Gao et al., 2017) that accounts for ~6.8% of the total area in China (Ma et al., 2011). Some of these lakes, such as Hulun Lake, play an irreplaceable role in maintaining biodiversity by protecting endangered species and migratory waterfowls (Liu et al., 2013; Tao et al., 2015), in addition to providing essential support for ecosystem services related to human well-being (Chen et al., 2012; Li et al., 2017). The last century has been a period of human activities combined with natural changes, especially rapid climate changes due to precipitation and temperature changes in recent decades, during which time global warming has greatly influenced changes in lakes, such as substantial lake shrinkage (Tao et al., 2015; Chen et al., 2018; Wang et al., 2018). Lake shrinkage poses significant threats, including dust release, water salinization, and waterfowl decline, to the regional environment and ecosystems (Ma et al., 2010; Liu et al., 2013; Zhang et al., 2017). Importantly, the climate of Inner Mongolia is influenced by the low-latitude East Asian summer monsoon (EASM), mid-latitude westerlies, and winter monsoon systems controlled by the Siberian High. The lake systems in this region are therefore sensitive to natural forcing factors and serve as valuable meteorological archives for revealing variations in the climate system (Chen et al., 2021).

China's natural grasslands, which cover 400 million hectares and account for 40% of the country's territory, not only play an important role in the construction of the national ecological environment, but also form the main basis of national ecological security and animal husbandry development in China (Yang et al., 2016). According to Chinese government reports, 10% of the total grassland area in China was degraded by the 1970s, with the degraded portion rising to 30% in the 1980s and to 50% in the mid-1990s. By the 2000s, ~90% of Chinese grasslands were degraded to varying degrees (Waldron et al., 2010).

Grassland ecosystems and lakes play an important role in supporting regional socioeconomic development. There is an inextricable link between the growth condition of grassland vegetation and change in lake water volume. In areas with strong vegetation water-supply capacity, the recharge of lake water by atmospheric precipitation and ice melt is stable, which ensures that the water volume of the lake changes with a stable or slightly increasing trend. However, in areas with poor vegetation water-holding

Corresponding authors: Liang Li; Email: lee911214@163.com; Boqiang Qin; Email: qinbq@niglas.ac.cn

Cite this article: Li L, Zhang Z, Ni Z, Sun W, Meng X, Zhang E, Zhu G, Zhang Y, Qin B (2024). Changes in the lake-grassland ecosystem revealed by multiple proxies in a sediment core from Ganggeng Nur Lake, northern China. *Quaternary Research* **117**, 30–42. https://doi.org/10.1017/qua.2023.27

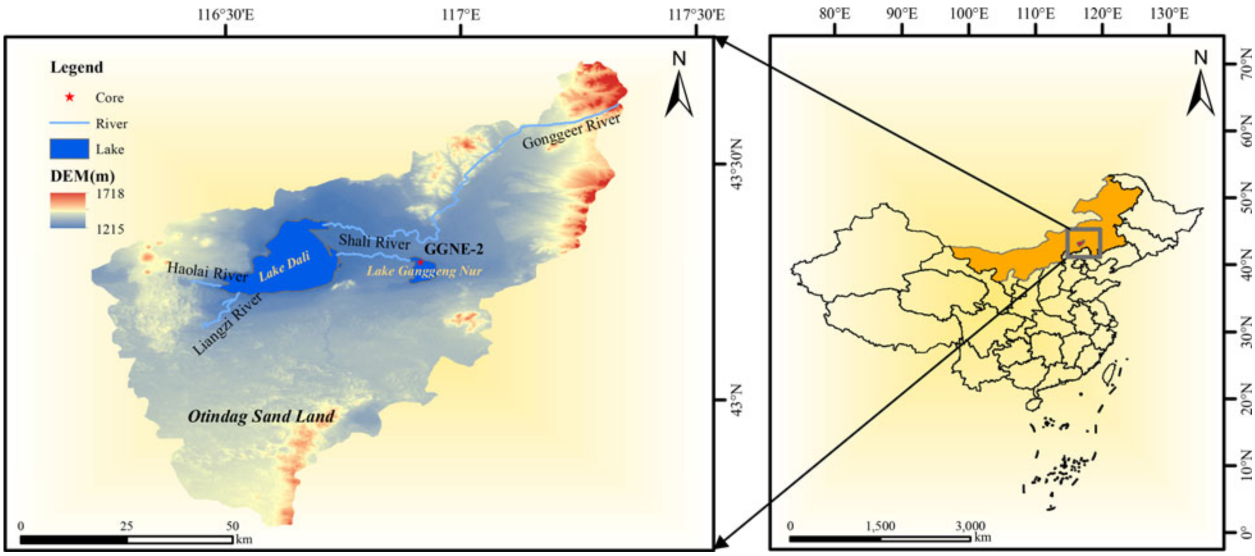

Figure 1. Location of Ganggeng Nur Lake in northern China and DEM (Digital Elevation Model) of the surrounding area. The sediment core sampling site in Ganggeng Nur Lake is indicated by the red star.

capacity, seasonal rainfall or glacial meltwater will increase the total water volume of the lake and its coastal wetlands in the short term, but due to the low vegetation cover and poor water-holding capacity around the lake, the soil will erode and cause vegetation degradation as soil sinks into the lake.

However, the evolution of lake-grassland ecosystems in recent centuries remains unclear due to the dearth of high-resolution records. The Dali Lake Basin mainly consists of Dali Lake, Ganggeng Nur Lake, and several rivers. The area of Dali Lake shrunk from 225 km^2 in 1983 to 191 km^2 in 2018 (Li et al., 2021). Grassland ecosystems also show varying degrees of degradation. In recent years, many studies have provided valuable references for studying climate and environmental changes in Dali Lake (Liu et al., 2016; Fan et al., 2019; Zhen et al., 2021; Zhang et al., 2023). However, most of these studies have focused on millennial- to centennial-scale environmental changes during the Holocene or the last deglaciation in the region, and there is a paucity of information from the last century, when human activities were most intense.

In this study, we use a sediment core from the freshwater Ganggeng Nur Lake in the Dali Lake Basin, in Chifeng City, Inner Mongolia (Fig. 1). We constructed a chronological framework from ^{210}Pb and ^{137}Cs dating and used multiple proxies of pollen, sediment grain size, and n-alkanes for comparative analysis to construct the climatic and environmental ecological changes on the scale of the past century. These results will be of great significance to the future ecological environment evaluation and resource utilization in this region, and will provide a reliable palynological study in revealing centennial- and decadal-scale changes of vegetation, climate, and human activities.

STUDY AREA

Ganggeng Nur Lake is located in Heshigten Banner, Chifeng City (116°53′29″E–116°57′52″E, 43°15′52″N–43°18′42″N), Inner Mongolia Autonomous Region, which is part of the Mengxin Plateau region, with a temperate continental monsoon climate and a frost-free period of 60–150 days/year. The lake area is ~21.5 km^2, with an average depth of 1.7 m, and an altitude of 1247 m. Ganggeng Nur Lake is on the northern margin of Otindag Sand Land and is mainly fed by the Shali River.

According to 1960–2020 meteorological data from the Chifeng City Meteorological Station, the average annual temperature of Ganggeng Nur Lake is 7.5°C, with an average temperature of −8°C in winter (December–February) and 22.3°C in summer (June–August), and the multiyear average precipitation is 361.2 mm, with an average summer precipitation of 248.8 mm, accounting for ~69% of the total annual precipitation (Fig. 2).

The modern vegetation type of the Ganggeng Nur Lake region is grassland vegetation. The main vegetation types of the alkaline soils around Ganggeng Nur Lake are *Phragmites australis*, *Tephroseris palustris*, *Typha latifolia*, *Hippuris vulgaris*, *Myriophyllum verticillatum*, and others. The grassland vegetation types are mainly Eurasian steppe plants, such as *Stipa grandis*, mostly belonging to Asteraceae, Poaceae, Fabaceae, Rosaceae, Ranunculaceae, and others (Mo et al., 2019).

MATERIALS AND METHODS

Sediment core sampling

A 34-cm core, GGNE-2 (43°17′34.38″N, 116°54′51.04″E), was collected by a gravity corer from Ganggeng Nur Lake at a water depth of 2.2 m in July 2018. The sediment core was sliced at 1 cm intervals, wrapped in sterile plastic bags, and stored in the laboratory refrigerator. The entire core lithology is black clay.

Dating and environmental parameter analysis

The GGNE-2 core ^{210}Pb and ^{137}Cs dating and analyses of sediment grain size, n-alkanes, and pollen were carried out at 1-cm resolution. Of these, ^{210}Pb, ^{137}Cs, grain-size analyses, and n-alkanes were carried out at the State Key Laboratory of Lake Science and Environment, Nanjing Institute of Geography and Limnology, Chinese Academy of Sciences; pollen analysis was carried out at the Palynology and Paleoecology Laboratory of Nanjing University, Nanjing, China.

https://doi.org/10.1017/qua.2023.27 Published online by Cambridge University Press

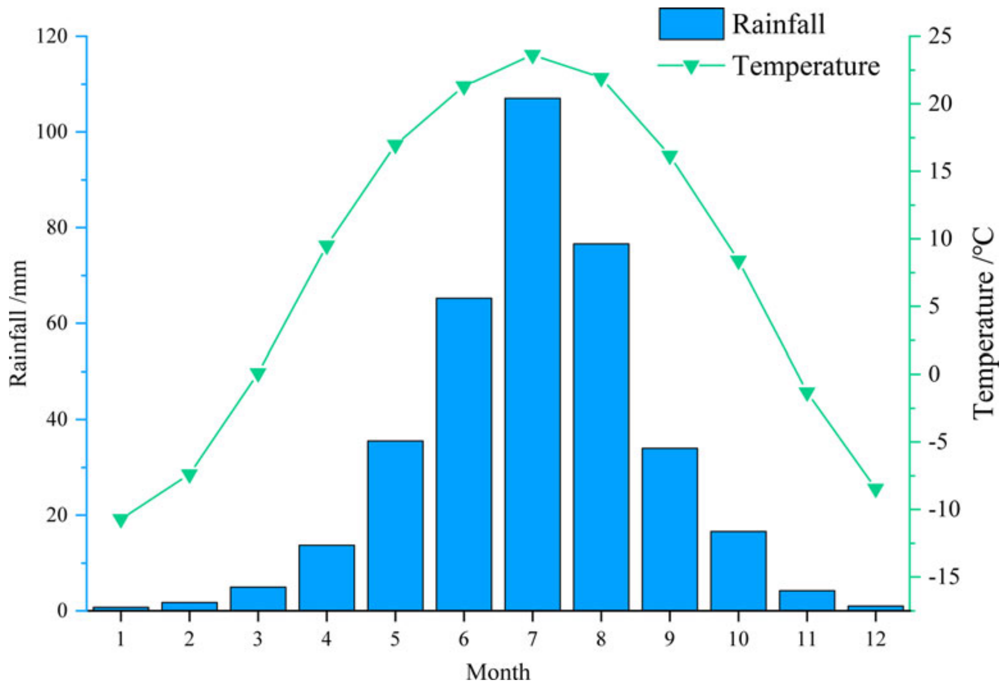

Figure 2. Climate diagram showing average monthly temperature and precipitation at the Chifeng City meteorological station from AD 1960–2020.

^{210}Pb and ^{137}Cs dating

The age model based on ^{210}Pb and ^{137}Cs was computed with the *serac* R package (https://github.com/rosalieb/serac; Bruel and Sabatier, 2020). The *serac* package uses the CRS (constant rate of supply) piecewise model, which simulates data from the CRS model combined with ^{137}Cs values to identify the depth of the peak. The age-depth curves of the CIC (constant initial concentration), CFCS (constant flux constant sedimentation rate), CRS, and CRS piecewise models can be calculated and plotted based on measured ^{210}Pb and ^{137}Cs data to construct the best age-depth framework (Bruel and Sabatier, 2020).

Sediment grain size analysis

Approximately 0.5 g was taken from each sample. Then, 10% H_2O_2 was used to remove organic matter, and 10% HCl was used to remove carbonate. Then, 10 ml of 10% $Na(PO_3)_6$ solution was added as a dispersing agent. Finally, the sediment grain size distributions were measured using a Malvern Mastersizer 3000.

Extraction and analysis of n-alkanes

A 5 g (± 0.0001 g) subsample was extracted from each lyophilized sample and sonicated three times (15 min each) at 110°C with a mixture of 60 ml dichloromethane and methanol (9:1, v:v) and then concentrated for drying under nitrogen. Neutral lipids containing n-alkanes were extracted by n-alkane silica gel column chromatography using hexane. The n-alkanes were measured using an Agilent 8890 gas chromatography (GC) DB-5 GC column (30 m × 0.25 mm, 0.25 µm film thickness) with an external C_8–C_{30} standard for quantification.

We chose an index, the proportion of aquatic n-alkanes (Paq) (Ficken et al., 2000), calculated from the measured n-alkane data, which is defined as:

$$Paq = (C_{23} + C_{25})/(C_{23} + C_{25} + C_{29} + C_{31})$$

Pollen analysis

Thirty-four subsamples of ∼1 g each were collected for pollen analysis. One tablet of *Lycopodium* spores (27560 grains/tablet) was added to each subsample to calculate pollen concentration and pollen accumulation rate. All subsamples were then treated with 10% HCl to dissolve carbonate, 10% NaOH to dissolve organic fractions, and 40% HF to dissolve silicate, and then were filtered in an ultrasonic bath with a 7 µm sieve. Finally, the pollen concentrates were stored in glycerol. Pollen taxa were identified under a ZEISS light microscope at × 400 magnification, and at least 500 grains of terrestrial plant taxa were counted for each subsample. Identification was aided by published literature (Xi and Ning, 1994; Jankovská and Komárek, 2000; Tang et al., 2016).

The percentage of terrestrial pollen was calculated from the total terrestrial pollen taxa, while pollen percentages of wetland and aquatic herbs and algae were calculated using the sum of all pollen and spore taxa (Xiao et al., 2020). The pollen diagram was plotted using Tilia 2.6.1 (Grimm, 2004). CONISS was used to identify pollen assemblage zones (Grimm, 1987).

RESULTS

Sediment chronology

We analyzed the GGNE-2 ^{210}Pb and ^{137}Cs data using the *serac* package. The results (shown in Fig. 3) indicated that the overall fluctuation of ^{210}Pb in Ganggeng Nur Lake was small, with a peak value of 476.2 Bq/kg. The sediment accumulation rate (SAR) in GGNE-2 was 7.07 mm/year. Depths of 18 cm and 24 cm (these correspond to 17.5 cm and 23.5 cm, respectively, in Fig. 3, due to the setting in the model) were selected as the depths corresponding to the ^{137}Cs outbreaks in 1986 and 1963, respectively, based on the chronological data from the CRS

https://doi.org/10.1017/qua.2023.27 Published online by Cambridge University Press

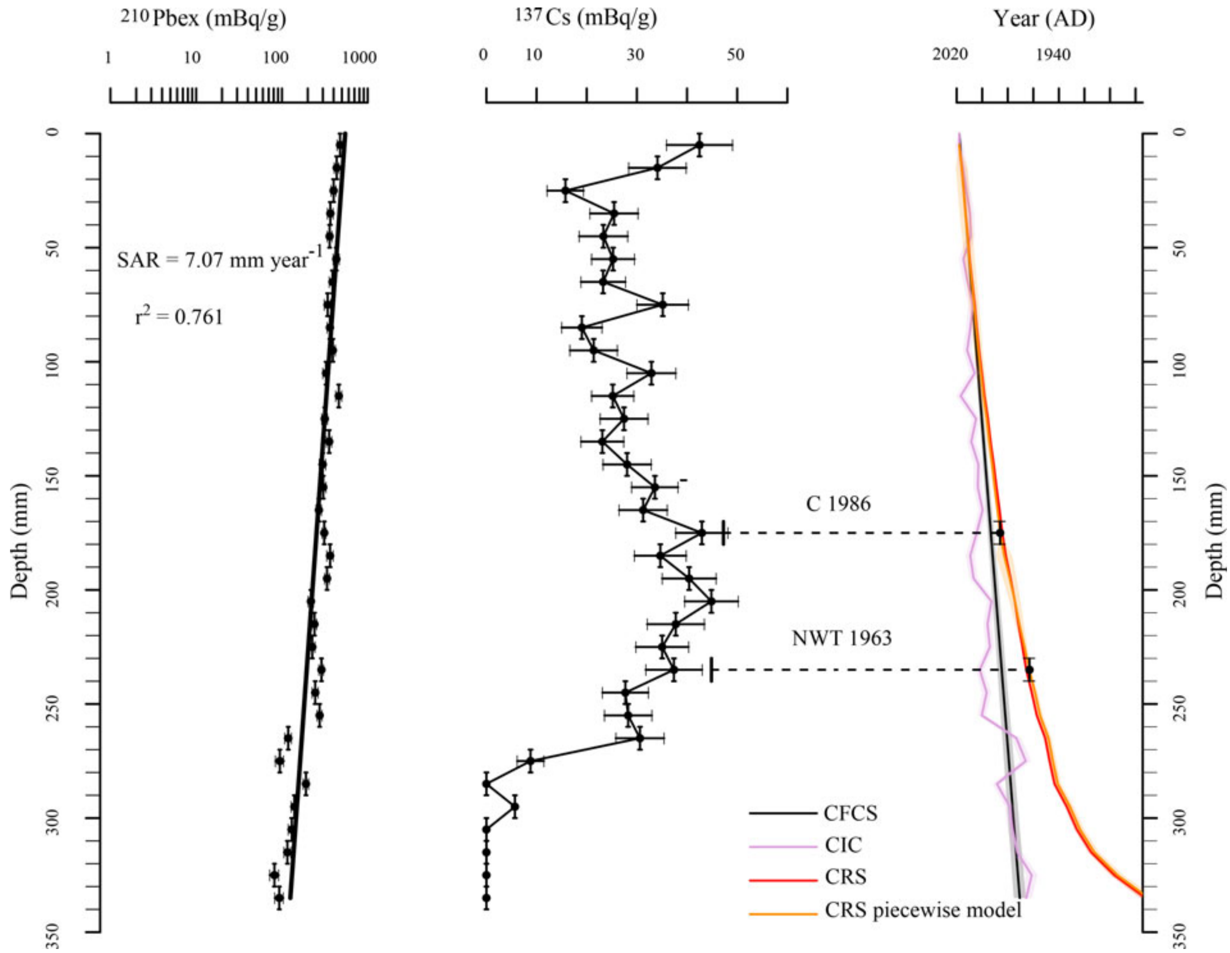

Figure 3. The age-depth framework of core GGNE-2 based on ^{210}Pb and ^{137}Cs dating. The ^{137}Cs outbreaks in 1986 and 1963 are indicated at depths of 18 cm and 24 cm, respectively. ^{210}Pbex = excess ^{210}Pb; NWT = nuclear weapons text peak; C = Chernobyl peak. Abbreviations used by the *serac* package: CRS = constant rate of supply; CIC = constant initial concentration; CFCS = constant flux constant sedimentation rate.

model and the peak value of ^{137}Cs. The piecewise model was used to finalize the GGNE-2 age-depth framework. Based on this, we provide a discussion of the climatic and ecological changes in Ganggeng Nur Lake over the past 150 years.

Sediment grain size

Sediment grain size over the last 150 years was classified and plotted according to the designations of clay (<4 μm), silt (4–64 μm), sand (>64 μm), median size and mean size (Fig. 4).

The clay fraction ranged from 6.2–23.3%, with a mean of 16.1%; the silt fraction ranged from 63.5–78.5%, with a mean of 73.7%; and the sand fraction ranged from 2.3–25.7%, with a mean of 10.2%. The median size varied from 10.2–33.4 μm, with a mean of 17.1 μm; the mean size ranged from 8.7–28.4 μm, with a mean of 13.7 μm (Fig. 4). The main component of GGNE-2 by grain size was silt. The trends of clay and sand variation were opposite, while the median and mean grain sizes were consistent with the sand content variation, indicating that the GGNE-2 sediment grain size was mainly influenced by sand variation.

The variation in each of the grain-size components is evident. The sand, median size, and mean size contents were higher, and the clay content was lower prior to AD 1945, while the sand, median size, and mean size contents decreased, and the clay content increased after AD 1945.

Pollen data

Forty-one terrestrial pollen taxa, three aquatic pollen taxa, and one algae taxon (*Pediastrum*) were identified in the GGNE-2 core (Fig. 5). The main terrestrial pollen taxa were *Pinus*, *Corylus*/*Carpinus*, *Betula*, *Alnus*, Poaceae, *Artemisia*, *Aster*, Brassicaceae, Apiaceae, Ranunculaceae, *Humulus*, Caryophyllaceae, Lamiaceae, Chenopodiaceae, and Cyperaceae, while the aquatic pollen taxa were mainly *Typha* and *Myriophyllum*. The terrestrial plants of the GGNE-2 core were characterized by *Pinus*, Chenopodiaceae, and *Artemisia*. Pollen records can be divided into four zones according to CONISS, the major pollen percentage diagram, and A/C (Fig. 5).

Zone 1: the natural evolution stage (AD 1870–1945, 34–28 cm)

In this zone, the proportion of upland herbs is the highest (~85.5%), dominated by *Artemisia* and Chenopodiaceae; the proportion of trees and shrubs is ~14.5%. The proportion of wetland herbs (Cyperaceae) is ~3.5% and the proportion

https://doi.org/10.1017/qua.2023.27 Published online by Cambridge University Press

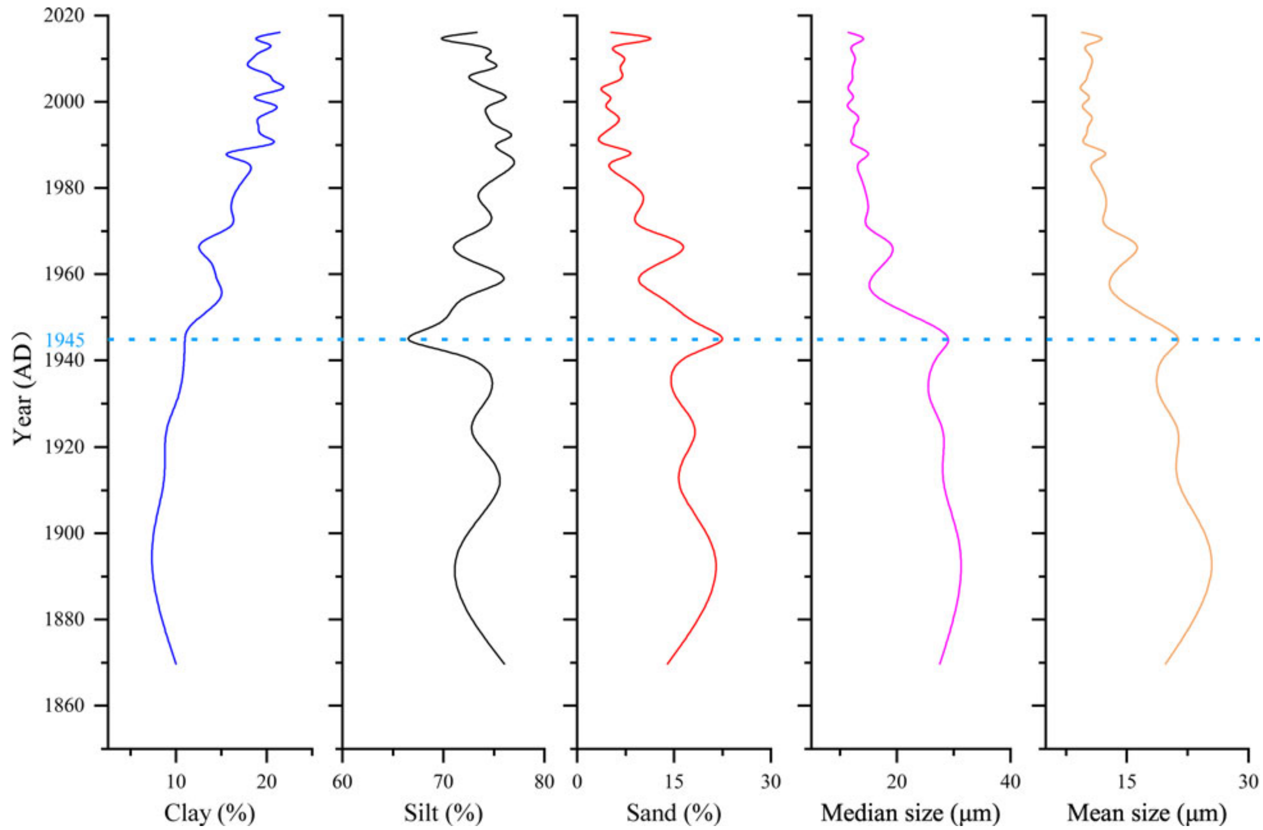

Figure 4. Grain-size distribution of core GGNE-2 in Ganggeng Nur Lake. Note grain size change before and after AD 1945.

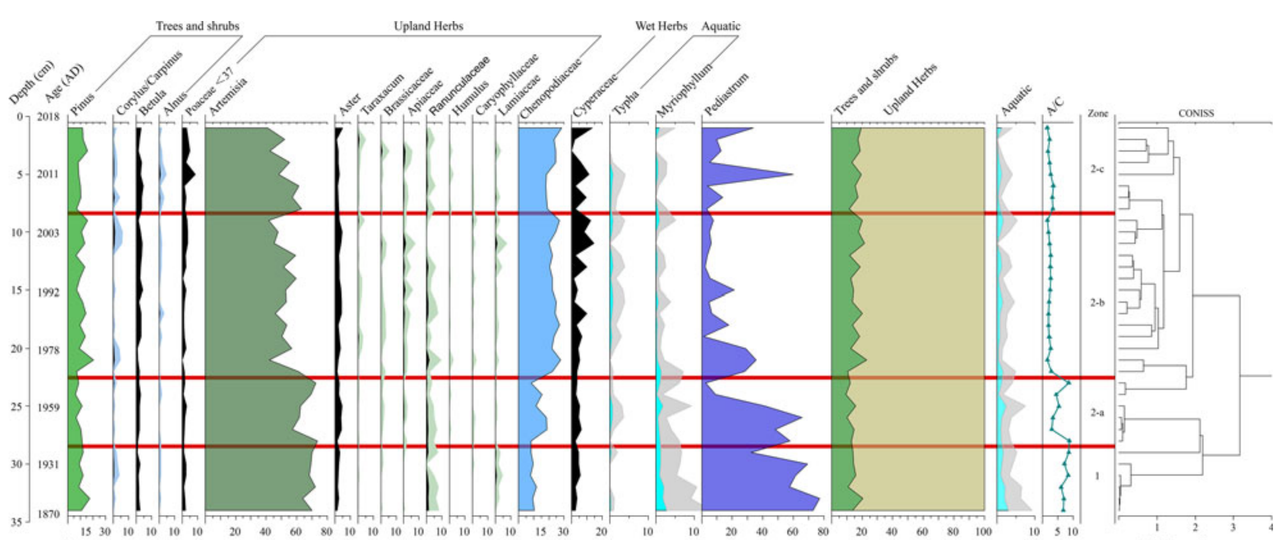

Figure 5. Diagram of pollen percentages and A/C (*Artemisia*/Chenopodiaceae) in core GGNE-2. Shadows show the exaggerations of the percentage data to make the key taxa more visible. Zone boundaries indicated by red, horizontal lines. Zone 1 = natural evolution stage (AD 1870–1945); Zone 2-a = human disturbance stage (AD 1945–1967); Zone 2-b = human transformation stage (AD 1967–2005); Zone 2-c = posttreatment stage (AD 2005–2018). Poaceae <37 = Poaceae <37 μm.

of aquatic plants is ~1.8%, of which *Myriophyllum* is the largest (~1.7%); *Pediastrum* has a higher proportion of the total (~61.2%). Zone 1 is characterized by the highest percentage of *Artemisia* (~69.5%), the lowest percentage of Chenopodiaceae (~9.4%), and a high percentage of *Pinus* (11.8%).

Zone 2-a: the human disturbance stage (AD 1945–1967, 28–23 cm)

In this zone, the percentage of upland herbs (87.5%), trees and shrubs (12.5%) change little; the percentage of wetland herbs (Cyperaceae) increases to 4.5%; the percentages of *Myriophyllum* (0.9%) and *Pediastrum* (~33.4%) decrease.

Among the three dominant terrestrial taxa, *Artemisia*, Chenopodiaceae, and *Pinus*, the content of *Pinus* (8.8%) and *Artemisia* (64.6%) start to show a decreasing trend, while the content of Chenopodiaceae (14.5%) increases. However, the percentage of *Artemisia* is still ~50%, which is higher than in either Chenopodiaceae or *Pinus*.

Zone 2-b: the human transformation stage (AD 1967–2005, 23–9 cm)

The proportion of upland herbs is slightly lower in this zone (83.6%). The proportions of trees and shrubs (16.4%) and wetland herbs (Cyperaceae, 6.2%) increase, while *Myriophyllum* (0.5%), and *Pediastrum* (12.5%) decline.

Artemisia, Chenopodiaceae, and *Pinus* were still the dominant terrestrial taxa in this zone. The content of *Artemisia* shows a continuously decreasing trend and reaches the lowest value (51.5%), while the content of Chenopodiaceae increases and reaches an unprecedented high value (23.6%). *Pinus* also shows an increasing trend (11.6%).

Zone 2-c: the posttreatment stage (AD 2005–2018, 9–0 cm)

The proportions of trees and shrubs (16.6%), upland herbs (83.4%), wetland herbs (Cyperaceae, 5.9%), and aquatic plants (0.7%) change little, while *Pediastrum* increases in this zone (17.9%). Among the three dominant terrestrial taxa in this zone, *Artemisia*, Chenopodiaceae, and *Pinus*, the percentage of Chenopodiaceae (21.8%) and *Pinus* (10.5%) decline while *Artemisia* (52.5%) increases.

Distribution of n-alkanes

A range of n-alkanes (nC_{17}–nC_{33}) was detected in the GGNE-2 core. Many studies have classified n-alkanes into three categories according to chain length: long-chain n-alkanes, medium-chain n-alkanes, and short-chain n-alkanes. Long-chain alkanes are defined as n-alkanes with carbon numbers greater than 26, short-chain n-alkanes are concentrated in n-alkanes with carbon numbers less than 21, and n-alkanes with carbon numbers between long-chain and short-chain are defined as medium-chain n-alkanes (Ficken et al., 2000; Sojinu et al., 2012; Fang et al., 2014). Variation in the percentages of short-chain (nC_{17}–nC_{20}), medium-chain (nC_{21}–nC_{26}), and long-chain (nC_{27}–nC_{33}) n-alkanes with age are shown in Figure 6.

The proportion of short-chain n-alkanes ranged from 4.8–12.6% with a mean of 7.2%; medium-chain n-alkanes ranged from 35.4–58.4% with a mean of 43.4%; and long-chain n-alkanes ranged from 33–59.7% with a mean of 49.9%. GGNE-2 was dominated by medium-chain and long-chain n-alkanes with a slight variation in short-chain n-alkanes.

Two stages can be distinguished based on changes in the content of the individual n-alkane components: (1) high content of short-chain (8.5%) and medium-chain (52.5%) n-alkanes with low content of long-chain n-alkanes (39%) before AD 1945, and (2) increased content of long-chain n-alkanes (52.3%) while the content of short-chain (6.8%) and medium-chain n-alkanes (40.9%) decreased after AD 1945.

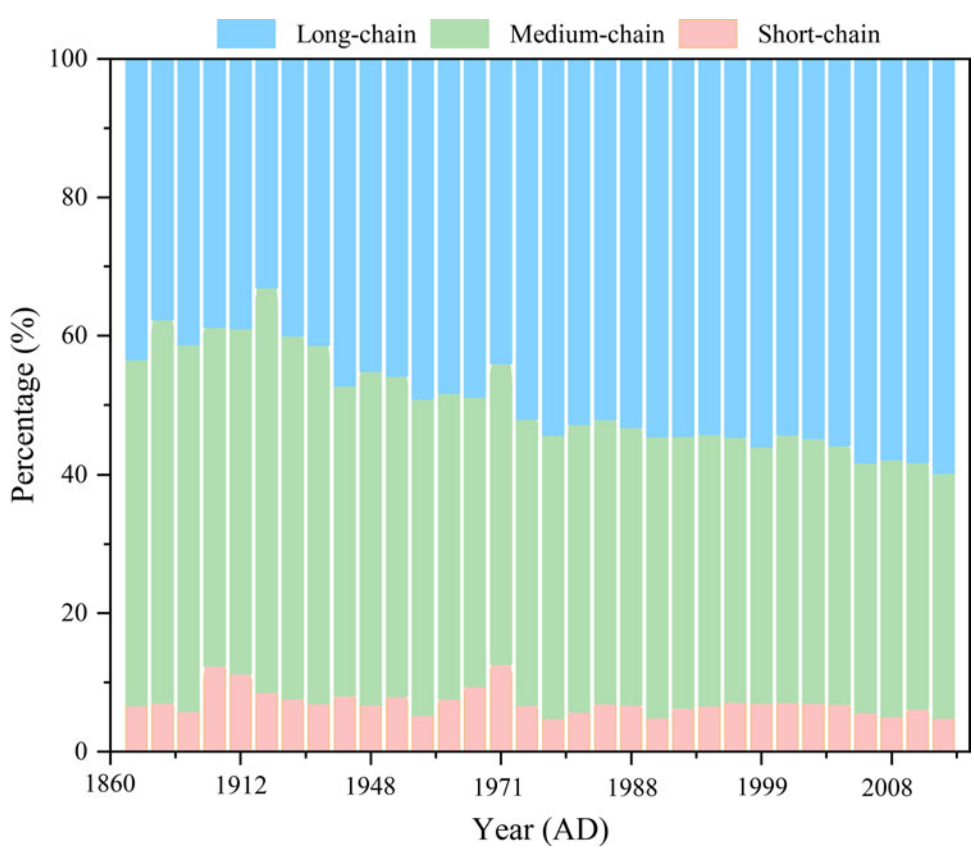

Figure 6. The proportions of n-alkanes in sediment core GGNE-2.

https://doi.org/10.1017/qua.2023.27 Published online by Cambridge University Press

DISCUSSION

Paleoenvironmental significance of environmental proxies in Ganggeng Nur Lake

In lacustrine sediment studies, different grain sizes in different regions imply different environmental changes, including changes in regional precipitation (Fan et al., 2021; Li et al., 2021), lake level fluctuation (Xiao et al., 2009, 2013; Dong et al., 2022), dust storms (Chen et al., 2020), and glacial advance and retreat (X. Zhang et al., 2021). Furthermore, what lacustrine sediment grain size indicates about the environment is not the same at different timescales and resolutions (Chen et al., 2004). It is generally accepted that in long-term, low-resolution sequences (centennial and millennial scales), coarse grain size indicates low lake water levels, reflecting an arid climate, while fine grain size indicates high lake water levels, reflecting a wet climate (Xiao et al., 2009; Fan et al., 2021). In contrast, the available interpretations for short-term, high-resolution (interannual, decadal) series are that coarse grain size indicates more precipitation and a wetter climate, and that fine grain size indicates less precipitation and a dryer climate (Liu et al., 2003; Zhang et al., 2003; Chen et al., 2004; Wang et al., 2011; Li et al., 2014). However, the climatic significance of coarse and fine grain sizes varies depending on the lake area, topography, watershed vegetation cover, and other influencing factors.

Considering the small area of Ganggeng Nur Lake, coupled with the confluence of the Shali River into the lake, an increase in precipitation on a short time scale would cause surface runoff to develop, and the stronger mechanical transport could bring coarse grains into the lake basin where they would settle, leading to coarser sediment grains. We interpret the grain size change in Ganggeng Nur Lake simply to indicate regional precipitation change as well as the lake water level.

N-alkanes are common components of plant waxes and can originate from algae, bacteria, phytoplankton, macrophytes, and terrestrial vascular plants (Ratnayake et al., 2006; Fang et al., 2014; Wang et al., 2015; Seopela et al., 2020). The proportion of aquatic n-alkanes (Paq) is an index based on n-alkanes that assesses the relative contribution of submerged/floating aquatic plants to terrestrial plants in lacustrine sediments (Ficken et al., 2000). Studies of Paq in lacustrine sediments have shown that Paq is sensitive to water depth and can be used to reflect fluctuations in lake water levels (Jiang et al., 2021). A high Paq suggests an association with lake expansion due to high precipitation, resulting in the input of large submerged/floating aquatic macrophytes into lacustrine sediments, while a low Paq indicates low precipitation and lake shrinkage, resulting in less aquatic plant input (Sun et al., 2013; Chu et al., 2014).

Arid and semiarid regions are sparsely vegetated, and grassland vegetation generally grows mainly in riparian environments

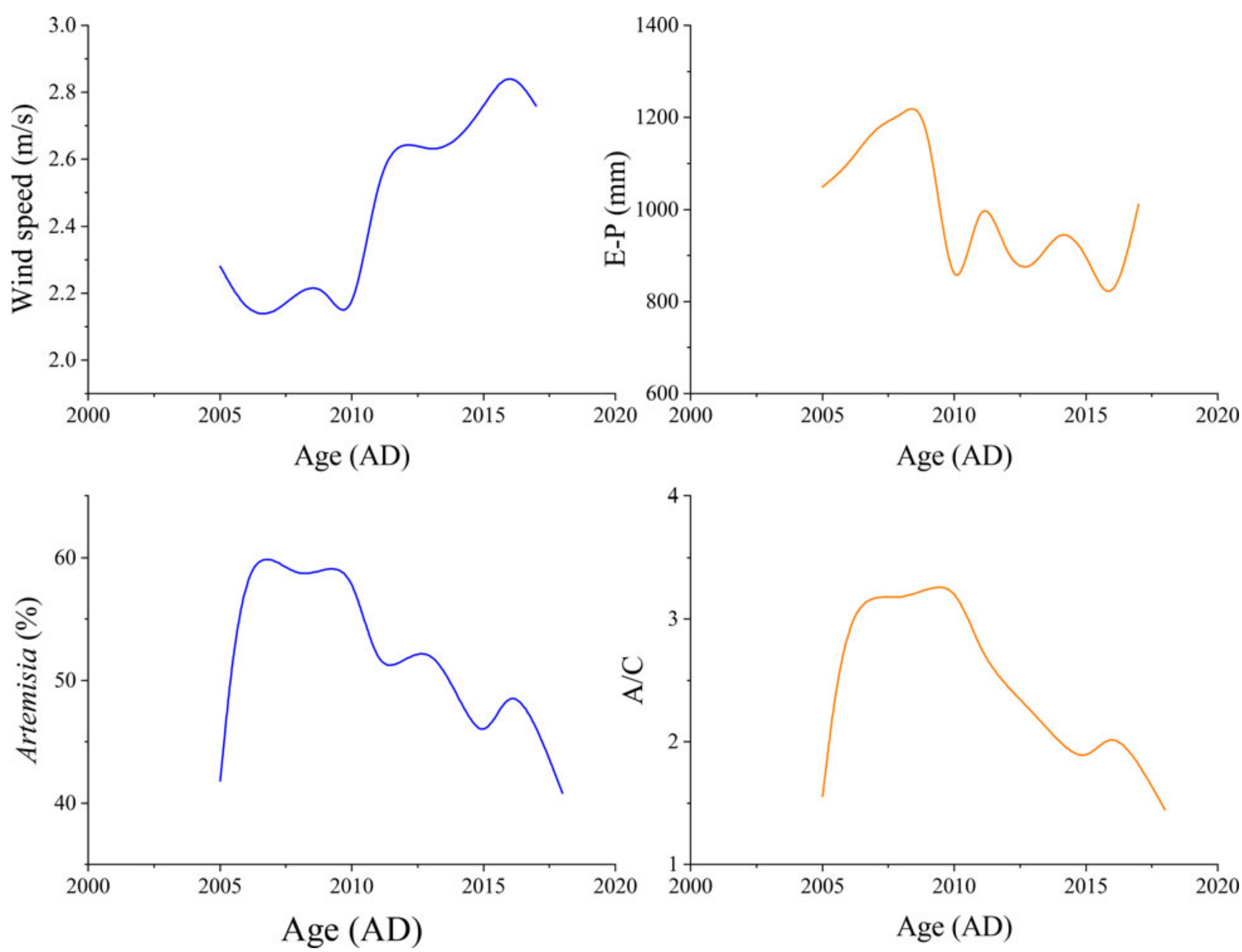

Figure 7. Comparison of wind speed, E−P(difference of evaporation and precipitation) at the Chifeng City meteorological station, *Artemisia* pollen content, and A/C in core GGNE-2, from AD 2005–2018.

(Gong et al., 2007; Metrak et al., 2015). Among the vegetation taxa, *Artemisia* and Chenopodiaceae are the dominant herbaceous taxa in arid and semiarid areas. Since *Artemisia* requires more moisture than Chenopodiaceae during the growing season, the *Artemisia*-Chenopodiaceae ratio (A/C) can be used in arid and semiarid areas to indicate dry-wet variation. A/C was proposed by El-Moslimany (1990), who pointed out that A/C needs to be used with caution and can only be applied within narrow geographical limits and within non-forested areas. Zhao (2012) found that A/C is applicable to study areas with annual precipitation <500 mm and where the summed percentage of *Artemisia* and Chenopodiaceae is greater than 45–50%. The annual precipitation in the area of Ganggeng Nur Lake is 361.2 mm, which is less than 500 mm, and the sum of *Artemisia* and Chenopodiaceae in the GGNE-2 core is 76%, which is much higher than 50%. The percentage of arboreal

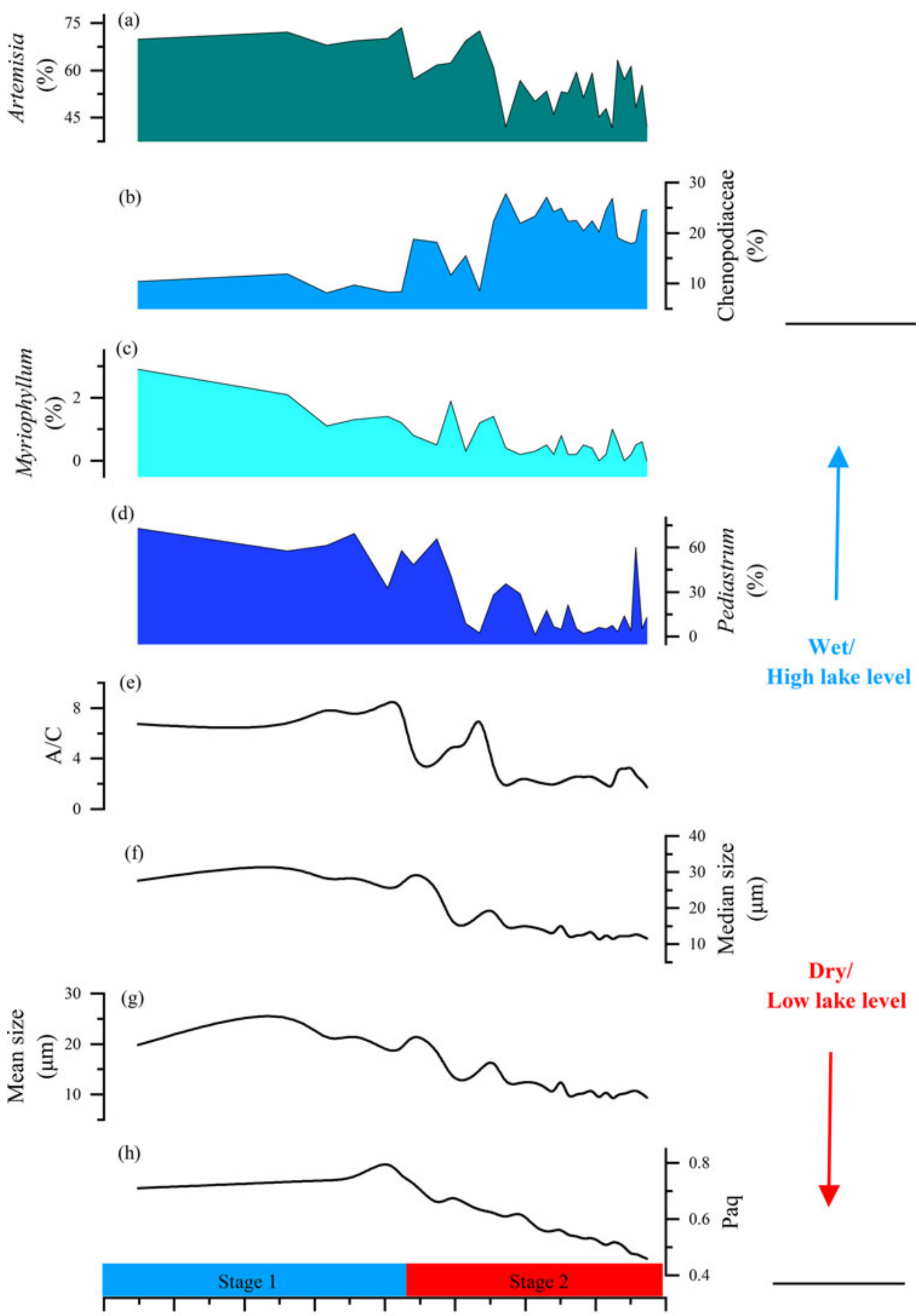

Figure 8. Comparison of various environmental proxies in core GGNE-2. (**a–d**) Percentages of *Artemisia*, Chenopodiaceae, *Myriophyllum* pollen, and *Pediastrum*; (**e**) A/C (*Artemisia*/Chenopodiaceae); (**f, g**) median size and mean size, respectively; (**h**) proportion of aquatic n-alkanes (Paq).

https://doi.org/10.1017/qua.2023.27 Published online by Cambridge University Press

pollen in the GGNE-2 core is very low (<20%), which indicates that there is no forest near the study site. In conclusion, A/C can be used to give a qualitative indication of humidity variation in Ganggeng Nur Lake.

Pediastrum is a common genus of green algae that grows mainly in freshwater environments, especially in ponds, swamps, and lakes (Whitney and Mayle, 2012; Wu et al., 2015a). Related studies have shown that the abundance of *Pediastrum* increases with increasing lake water level (Zhao et al., 2007; Turner et al., 2016). *Myriophyllum* is a genus of aquatic plants that is often found in standing or slow-moving water environments (Hussner et al., 2009). In aquatic ecosystems, *Myriophyllum* pollen can be used to infer water-level fluctuations in shallow lakes (Shulmeister and Lees, 1995; Prebble et al., 2005). CCA (Canonical Correspondence Analysis) analysis of pollen from cores in Baiyangdian Lake showed that water level was more closely related to *Myriophyllum*, with increases in *Myriophyllum* pollen content indicating deeper lake water (Guo et al., 2012). The general trends of *Pediastrum* and *Myriophyllum* in the GGNE-2 core were consistent with *Artemisia* and opposite of Chenopodiaceae, therefore we suggest that *Pediastrum* and *Myriophyllum* can be simple indicators of changes in lake water level here.

Since *Artemisia* pollination is anemophilous, short-term changes in *Artemisia* content are influenced by wind speed. Based on this, we selected wind speed, the difference between evaporation and precipitation (E−P) in meteorological data for Chifeng City (which indicates humidity), A/C, and the percentage of *Artemisia* in core GGNE-2 for comparison from AD 2005–2018 (Fig. 7). The percentage of *Artemisia*, A/C, and wind speed show a clear inverse relationship and a better positive relationship with E−P, which indicates that vegetation changes in this stage were influenced by the combined effect of wind speed and humidity.

Vegetation and paleoenvironmental reconstruction of Ganggeng Nur Lake

The vegetation and paleoenvironmental evolution of Ganggeng Nur Lake over the past 150 years were reconstructed (Figs. 5

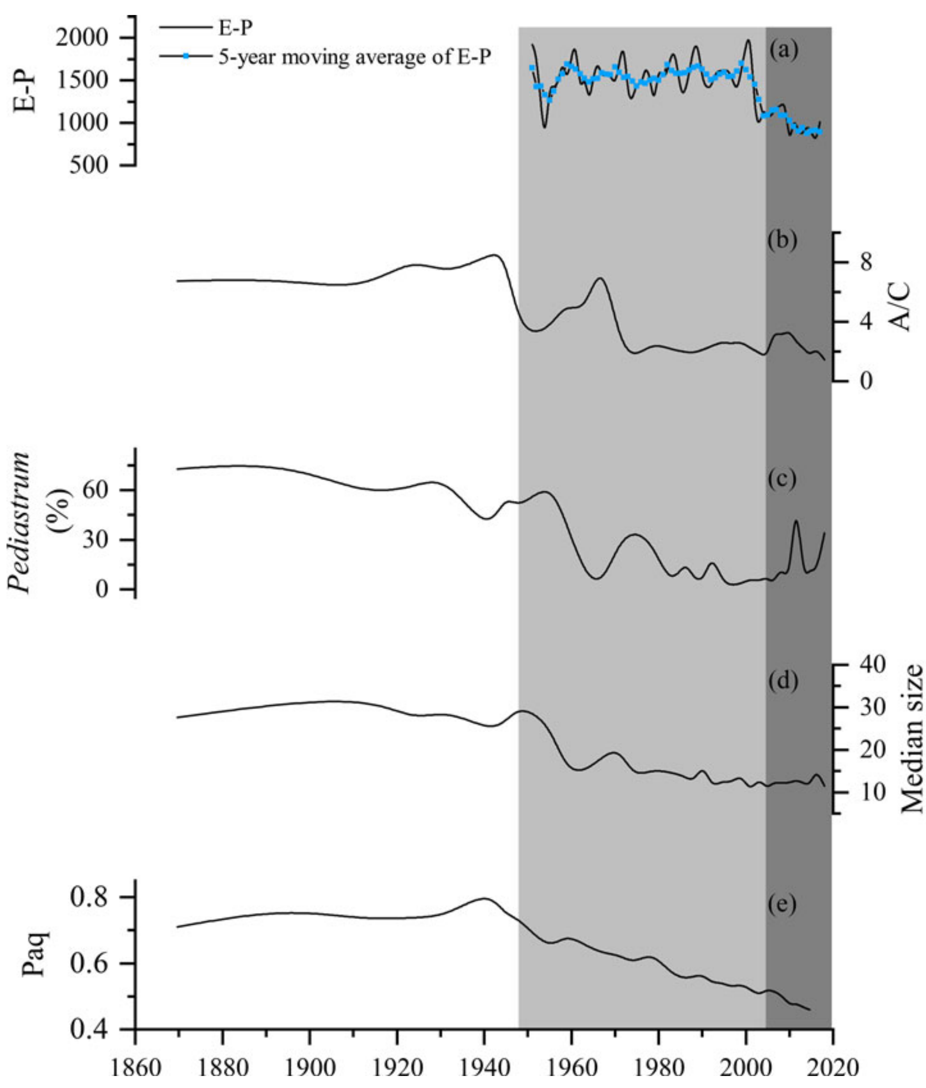

Figure 9. Comparison of records in core GGNE-2 and other indicators. (**a**) The difference between evaporation and precipitation (E−P) and its five-year moving average for Chifeng City; (**b**) A/C in sediment core GGNE-2; (**c**) proportion of *Pediastrum* in sediment core GGNE-2; (**d**) median size in sediment core GGNE-2; (**e**) proportion of aquatic n-alkanes (Paq) in sediment core GGNE-2. Vertical shaded area on the left represents AD 1945 to AD 2005; vertical shaded area on the right = AD 2005 to AD 2018.

and 8) and are discussed below in the sections on the recognized stages in the area.

Stage 1: the natural evolution stage (AD 1870–1945, 34–28 cm)
The contents of *Artemisia*, *Myriophyllum*, and *Pediastrum* reached the highest values with the coarse grain size, high A/C, and Paq, indicating that the vegetation type of Ganggeng Nur Lake was grassland, coupled with a humid climate and high lake level. *Artemisia* was the main dominant species in this stage.

Stage 2 (AD 1945–2018, 28–0 cm)
The proportions of *Artemisia*, *Myriophyllum*, and *Pediastrum* showed a decreasing trend with the fine grain size, low A/C, and Paq compared to Stage 1. The proportion of *Artemisia* is still very high, indicating that the vegetation type of Ganggeng Nur Lake was grassland with *Artemisia* as the main dominant species in this stage, coupled with a dry climate and low lake level compared with Stage 1. Stage 2 can be further divided into three stages (Stage 2-a–2-c) based on *Myriophyllum*, *Pediastrum*, and A/C changes as follows (Fig. 5).

Stage 2-a: the human disturbance stage (AD 1945–1967, 28–23 cm) The content of *Artemisia*, *Myriophyllum*, *Pediastrum*, and A/C showed a slight decrease in Stage 2-a compared to their content in Stage 1. The proportion of *Artemisia* was still higher than Chenopodiaceae, indicating that *Artemisia* was still the main dominant genus for the grassland, and that the climate in this stage was in the wet-dry transition period.

Stage 2-b: the human transformation stage (AD 1967–2005, 23–9 cm) The lowest percentages of *Artemisia*, *Myriophyllum*, and *Pediastrum* with low A/C at the same time suggest that the climate in this area became dry and the lake level was low.

Stage 2-c: the posttreatment stage (AD 2005–2018, 9–0 cm) The ecosystem was still a grassland ecosystem where *Artemisia* and Chenopodiaceae were the dominant taxa. The proportion of *Artemisia* increased compared to in Stage 2-b, while Chenopodiaceae decreased, the aquatic plant *Myriophyllum* did not change much, and *Pediastrum* and A/C showed increasing trends compared to Stage 2-b, indicating that the climate became slightly wetter in Stage 2-c compared to Stage 2-b.

The chronological results obtained from the GGNE-2 core show that sediment was deposited during the modern period, which includes the modern instrumental observation period. Precipitation and evaporation data for the last 60 years in

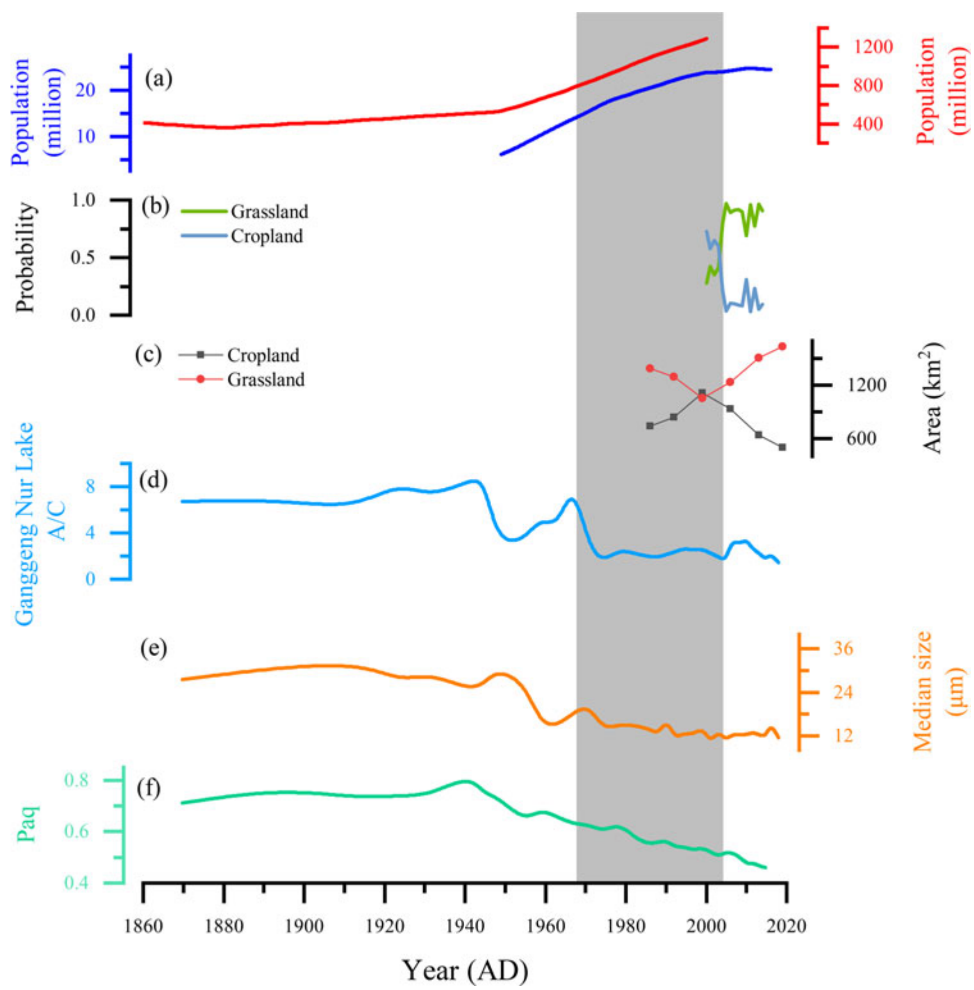

Figure 10. Comparison of Ganggeng Nur Lake proxies and other indicators. (**a**) The population of China over the past 150 years (red line, Jiang et al. 2022) and the population of Inner Mongolia since AD 1949 (blue line); (**b**) the utilization rate of cropland and grassland after cropland retirement in Inner Mongolia since AD 2000 (Yin et al., 2018); (**c**) the area of grassland and cropland in the Daihai Lake watershed over the past 40 years (Y. Zhang et al., 2021); (**d**) A/C in sediment core GGNE-2; (**e**) median size in sediment core GGNE-2; (**f**) proportion of aquatic n-alkanes (Paq) in sediment core GGNE-2. Vertical gray bar = AD 1967 to AD 2005.

https://doi.org/10.1017/qua.2023.27 Published online by Cambridge University Press

Chifeng City from the meteorological station were selected for analysis to verify the accuracy of the climatic environmental changes revealed by the proxies used in this study (Fig. 9). The difference between evaporation and precipitation (E−P) was calculated and used to represent the humidity change in this area.

E−P and its five-year moving average for Chifeng City show that the climate in Chifeng City was arid from the beginning of the modern instrumental record to AD 2005. After AD 2005, climate shifted to a more humid environment, which is consistent with the stage of climate change revealed by pollen. This suggests that pollen is comparatively more accurate in revealing changes in the climatic environment over the past 150 years.

Regional comparison and the effect of human activity

Because the last century has been a period of human activities combined with natural changes, the effect of human activities in Ganggeng Nur Lake over the last 150 years is inevitable. We selected the population of China in the last 150 years, the population of Inner Mongolia, China, since AD 1949, the utilization rate of cropland and grassland after cropland retirement in Inner Mongolia since AD 2000 (Yin et al., 2018), the area of grassland and cropland in the Daihai Lake watershed in the last 40 years (Y. Zhang et al., 2021), and the A/C, median size, and Paq indices of Ganggeng Nur Lake for comparison (Fig. 10).

Since the founding of the People's Republic of China, as the country recovered from the wounds of war, its economy began to recover, its population grew, and human activities gradually increased. From the establishment of the People's Republic of China in AD 1949 to the end of the twentieth century, an increasing number of natural grasslands in Inner Mongolia were converted into arable land due to the migration of agricultural populations from neighboring provinces and due to land reclamation policies for economic development (Wu et al., 2015b; Yin et al., 2018). Moreover, the Inner Mongolian government implemented the 'household contract responsibility system' from AD 1983 to the beginning of the twenty-first century, which made overgrazing the direct and main cause of large-scale grassland degradation (Wu et al., 2015b). Because grasslands play a role in water and soil conservation, large-scale grassland degradation led to large-scale soil erosion in Inner Mongolia. Coupled with the arid natural environment, environmental degradation was aggravated, and large amounts of silt accumulated, blocking rivers, and causing large-scale lake shrinkage. Given these conditions, China proposed the Grain for Green Project program in AD 1999 to control soil erosion and improve land quality in the face of economic development (Fu et al., 2017). The program, which has been used to improve soil erosion through terracing, afforestation, and restoration of grassland vegetation, already has achieved positive results in northern China.

The effect of human activities on Ganggeng Nur Lake is consistent with that of northern China. A series of measures led to the large-scale degradation of grasslands in Inner Mongolia and exacerbated the climate of Ganggeng Nur Lake, which began to shift to arid from AD 1945–1967; especially after AD 1967, Ganggeng Nur Lake was in a more arid state, and the lake water level was lower. Implementation of the Grain for Green Project program improved local soil erosion, which allowed the grassland vegetation to recover during this period, and the climate slowly became wetter, and the lake level became more stable.

CONCLUSIONS

A study of sediment in the GGNE-2 core using ^{137}Cs and ^{210}Pb dating, sediment grain size, pollen, n-alkanes, and instrumental data from Chifeng City, Inner Mongolia, reconstructed the lake-grassland ecosystem change in Ganggeng Nur Lake over the past 150 years. Overall, our study provides a reference case for short-scale, high-resolution changes in a localized lake-grassland ecosystem. The results showed that vegetation types of the grassland ecosystem of Ganggeng Nur Lake in the Dali Lake basin over the past 150 years were mainly dominated by *Artemisia*, Chenopodiaceae, and *Pinus*, and that the lake-grassland ecosystem can be divided into four stages.

Natural evolution stage (AD 1870–1945)—The lake-grassland ecosystem with *Artemisia* as the dominant vegetation species, in which the climate was humid, the water level of the lake was high, and the effect of human activities was low.

Human disturbance stage (AD 1945–1967)—This stage was early during the establishment of the People's Republic of China, when the population began to increase, human effect on the local environment increased, and the climate transitioned from humid to arid.

Human transformation stage (AD 1967–2005)—The content of *Artemisia* in the vegetation type at this stage reached its lowest value, the climate was arid, and the lake level was low. During this stage, China converted increasingly more grassland into arable land to develop the economy, and overgrazing-exacerbated soil loss. The effect of human activities exacerbated the arid climate and lowered the lake level, and the lake-grassland ecosystem of Ganggeng Nur Lake steadily deteriorated.

Posttreatment stage (AD 2005–2018)—During this stage, the content of *Artemisia* showed an increase in the vegetation types, and the overall climate became more humid. Implementation of the Grain for Green Project program improved the lake-grassland ecosystem of Ganggeng Nur Lake.

Acknowledgments. Thanks to Yiman Fang of Zhejiang University for help with the paper and to the reviewers for their professional advice. This research was funded by the National Natural Science Foundation of China (41790423).

REFERENCES

Bruel, R., Sabatier, P., 2020. *serac*: an R package for ShortlivEd RAdionuclide chronology of recent sediment cores. *Journal of Environmental Radioactivity* **225**, 106449. https://doi.org/10.1016/j.jenvrad.2020.106449.

Chen, B., Chen, L., Huang, B., Michishita, R., Xu, B., 2018. Dynamic monitoring of the Poyang Lake wetland by integrating Landsat and MODIS observations. *ISPRS Journal of Photogrammetry and Remote Sensing* **139**, 75–87.

Chen, C., Tao, S., Zhao, W., Jin, M., Wang, Z., Li, H., Ren, H., Li, G., 2021. Holocene lake level, vegetation, and climate at the East Asian summer monsoon margin: a record from the Lake Wulanhushao basin, southern Inner Mongolia. *Palaeogeography, Palaeoclimatology, Palaeoecology* **561**, 110051. https://doi.org/10.1016/j.palaeo.2020.110051.

Chen, F., Chen, S., Zhang, X., Chen, J., Wang, X., Gowan, E.J., Qiang, M., *et al.*, 2020. Asian dust-storm activity dominated by Chinese dynasty changes since 2000 BP. *Nature Communications* **11**, 992. https://doi.org/10.1038/s41467-020-14765-4.

Chen, J.A., Wan, G., Zhang, D.D., Zhang, F., Huang, R., 2004. Environmental records of lacustrine sediments in different time scales: Sediment grain size as an example. *Science in China Series D: Earth Sciences* **47**, 954–960.

Chen, X., Chuai, X., Yang, L., Zhao, H., 2012. Climatic warming and overgrazing induced the high concentration of organic matter in Lake Hulun, a large shallow eutrophic steppe lake in northern China. *Science of the Total Environment* **431**, 332–338.

Chu, G., Sun, Q., Xie, M., Lin, Y., Shang, W., Zhu, Q., Shan, Y., *et al.*, 2014. Holocene cyclic climatic variations and the role of the Pacific Ocean as recorded in varved sediments from northeastern China. *Quaternary Science Reviews* **102**, 85–95.

Dong, S., Li, Z., Li, M., Wang, N. A., Lu, C., Ning, K., 2022. Quantitative reconstruction of consecutive paleolake-level fluctuations by the groundwater recharged lake in the desert hinterland: a case study in the Badain Jaran Desert, Northwestern China. *Catena* **212**, 106051. https://doi.org/10.1016/j.catena.2022.106051.

El-Moslimany, A.P., 1990. Ecological significance of common nonarboreal pollen: examples from drylands of the Middle East. *Review of Palaeobotany and Palynology* **64**, 343–350.

Fan, J., Jiang, H., Shi, W., Guo, Q., Zhang, S., Wei, X., Xu, H., *et al.*, 2021. A 450-year warming and wetting climate in southern Altay inferred from a Yileimu Lake sediment core. *Quaternary International* **592**, 37–50.

Fan, J., Xiao, J., Wen, R., Zhang, S., Huang, Y., Yue, J., Wang, X., *et al.*, 2019. Mineralogy and carbonate geochemistry of the Dali Lake sediments: implications for paleohydrological changes in the East Asian summer monsoon margin during the Holocene. *Quaternary International* **527**, 103–112.

Fang, J., Wu, F., Xiong, Y., Li, F., Du, X., An, D., Wang, L., 2014. Source characterization of sedimentary organic matter using molecular and stable carbon isotopic composition of n-alkanes and fatty acids in sediment core from Lake Dianchi, China. *Science of the Total Environment* **473**, 410–421.

Feng, L., Han, X., Hu, C., Chen, X., 2016. Four decades of wetland changes of the largest freshwater lake in China: possible linkage to the Three Gorges Dam?. *Remote Sensing of Environment* **176**, 43–55.

Ficken, K.J., Li, B., Swain, D.L., Eglinton, G., 2000. An n-alkane proxy for the sedimentary input of submerged/floating freshwater aquatic macrophytes. *Organic Geochemistry* **31**, 745–749.

Fu, B., Wang, S., Liu, Y., Liu, J., Liang, W., Miao, C., 2017. Hydrogeomorphic ecosystem responses to natural and anthropogenic changes in the Loess Plateau of China. *Annual Review of Earth and Planetary Sciences* **45**, 223–243.

Gao, H., Ryan, M.C., Li, C., Sun, B., 2017. Understanding the role of groundwater in a remote transboundary lake (Hulun Lake, China). *Water* **9**, 363. https://doi.org/10.3390/w9050363.

Gong, X.M., Ma, Y., Gui, D.W., Yuan, Z.Y., Lu, G.H., 2007. The ecological fragility appraisal of the natural meadow in a typical basin of arid area. *Journal of the Chengdu University of Technology* (*Science & Technology Edition*) **34**, 216–220.

Grimm, E.C., 1987. CONISS: a FORTRAN 77 program for stratigraphically constrained cluster analysis by the method of incremental sum of squares. *Computers & Geosciences* **13**, 13–35.

Grimm, E.C., 2004. *TILIA and TILIA.GRAPH view version 2.0.2*. Illinois State Museum, Research and Collector Center, Springfield, Illinois.

Guo, T., Yang, Z. F., Chen, H., 2012. Pollen assemblages and their environmental correlates during the past 200 years inferred from sediments records in a shallow lake. *Procedia Environmental Sciences* **13**, 363–376.

Hussner, A., Meyer, C., Busch, J., 2009. The influence of water level and nutrient availability on growth and root system development of *Myriophyllum* aquaticum. *Weed Research* **49**, 73–80.

Jankovská, V., Komárek, J., 2000. Indicative value of *Pediastrum* and other coccal green algae in palaeoecology. *Folia Geobotanica* **35**, 59–82.

Jiang, H., Han, Y., Guo, M., Gong, X., 2022. Sedimentary records of human activities in China over the past two millennia and implications for the Anthropocene: a review. *Science of The Total Environment*, 158149. https://doi.org/10.1016/j.scitotenv.2022.158149.

Jiang, J., Meng, B., Liu, H., Wang, H., Kolpakova, M., Krivonogov, S., Song, M., Zhou, A., Liu, W., Liu, Z., 2021. Water depth control on n-alkane distribution and organic carbon isotope in mid-latitude Asian lakes. *Chemical Geology* **565**, 120070. https://doi.org/10.1016/j.chemgeo.2021.120070.

Li, H., Gao, Y., Li, Y., Yan, S., Xu, Y., 2017. Dynamic of Dalinor lakes in the Inner Mongolian Plateau and its driving factors during 1976–2015. *Water* **9**, 749. https://doi.org/10.3390/w9100749.

Li, H.Y., Ming, Q.Z., Zhang, H.C., Duan, L.Z., Zhang, Z.Q., 2014. Paleoclimatic significance of grain-size from lacustrine sediments in China. *Scientific Journal of Earth Science* **4**, 98–108.

Li, W., Wang, L., Zhang, Y., Wu, L., Zeng, L., Tuo, Z., 2021. Determining the groundwater basin and surface watershed boundary of Dalinuoer Lake in the middle of Inner Mongolian Plateau, China and its impacts on the ecological environment. *China Geology* **4**, 498–508.

Liu, H., Yin, Y., Piao, S., Zhao, F., Engels, M., Ciais, P., 2013. Disappearing lakes in semiarid northern China: drivers and environmental impact. *Environmental Science & Technology* **47**, 12107–12114.

Liu, S., Deng, C., Xiao, J., Li, J., Paterson, G.A., Chang, L., Yi, L., Qin, H., Zhu, R., 2016. High-resolution enviromagnetic records of the last deglaciation from Dali Lake, Inner Mongolia. *Palaeogeography, Palaeoclimatology, Palaeoecology* **454**, 1–11.

Liu, X., Wang, S., Shen, J., 2003. The grainsize of the core QH-2000 in Qinghai Lake and its implication for paleoclimate and paleoenvironment. *Journal of Lake Sciences* **15**, 112–117.

Ma, R., Duan, H., Hu, C., Feng, X., Li, A., Ju, W., Jiang, J., Yang, G., 2010. A half-century of changes in China's lakes: global warming or human influence?. *Geophysical Research Letters* **37**, L24106. https://doi.org/10.1029/2010GL045514.

Ma, R., Yang, G., Duan, H., Jiang, J., Wang, S., Feng, X., Li, A., *et al.*, 2011. China's lakes at present: number, area and spatial distribution. *Science China Earth Sciences* **54**, 283–289.

Metrak, M., Sulwinski, M., Chachulski, L., Wilk, M., Suska-Malawska, M., 2015. Creeping environmental problems in the Pamir Mountains: landscape conditions, climate change, wise use and threats. In: Öztürk, M., Hakeem, K., Faridah-Hanum, I., Efe, R. (Eds.), *Climate Change Impacts on High-Altitude Ecosystems*. Springer, Cham, pp. 665–694.

Mo, Y., Zheng, Y., Jin, F., Bao, Y., Jia, Z., 2019. Aerobic methane oxidation under distinct shrinkage scenario of Lake Ganggeng in Inner Mongolia Autonomous Region. *Acta Microbiologica Sinica* **59**, 1105–1115. [in Chinese]

Prebble, M., Sim, R., Finn, J., Fink, D., 2005. A Holocene pollen and diatom record from Vanderlin Island, Gulf of Carpentaria, lowland tropical Australia. *Quaternary Research* **64**, 357–371.

Ratnayake, N.P., Suzuki, N., Okada, M., Takagi, M., 2006. The variations of stable carbon isotope ratio of land plant-derived n-alkanes in deep-sea sediments from the Bering Sea and the North Pacific Ocean during the last 250,000 years. *Chemical Geology* **228**, 197–208.

Seopela, M. P., McCrindle, R. I., Combrinck, S., Augustyn, W., 2020. Occurrence, distribution, spatio-temporal variability and source identification of n-alkanes and polycyclic aromatic hydrocarbons in water and sediment from Loskop dam, South Africa. *Water Research* **186**, 116350. https://doi.org/10.1016/j.watres.2020.116350.

Shulmeister, J., Lees, B.G., 1995. Pollen evidence from tropical Australia for the onset of an ENSO-dominated climate at c. 4000 BP. *The Holocene* **5**, 10–18.

Sojinu, S.O., Sonibare, O.O., Ekundayo, O., Zeng, E.Y., 2012. Assessing anthropogenic contamination in surface sediments of Niger Delta, Nigeria with fecal sterols and *n*-alkanes as indicators. *Science of the Total Environment* **441**, 89–96.

Sun, Q., Xie, M., Shi, L., Zhang, Z., Lin, Y., Shang, W., Wang, K., Li, W., Liu, J., Chu, G., 2013. Alkanes, compound-specific carbon isotope measures and climate variation during the last millennium from varved sediments of Lake Xiaolongwan, northeast China. *Journal of Paleolimnology* **50**, 331–344.

Tang, L., Mao, L., Shu, J., Li, C., Shen, C, Zhou, Z., 2016. *An Illustrated Handbook of Quaternary Pollen and Spores in China*. Science Press, Beijing.

Tao, S., Fang, J., Zhao, X., Zhao, S., Shen, H., Hu, H., Tang, Z., Wang, Z., Guo, Q., 2015. Rapid loss of lakes on the Mongolian Plateau. *Proceedings of the National Academy of Sciences* **112**, 2281–2286.

Turner, F., Zhu, L., Lü, X., Peng, P., Ma, Q., Wang, J., Hou, J., Lin, Q., Yang, R., Frenzel, P., 2016. *Pediastrum* sensu lato (Chlorophyceae) assemblages from surface sediments of lakes and ponds on the Tibetan Plateau. *Hydrobiologia* **771**, 101–118.

Waldron, S., Brown, C., Longworth, J., 2010. Grassland degradation and livelihoods in China's western pastoral region: a framework for understanding and refining China's recent policy responses. *China Agricultural Economic Review*. **2**, 298–320.

Wang, R., Peng, W., Liu, X., Wu, W., Chen, X., Zhang, S., 2018. Responses of water level in China's largest freshwater lake to the meteorological drought index (SPEI) in the past five decades. *Water* **10**, 137. https://doi.org/10.3390/w10020137.

Wang, X.L., Yang, H., Zhao, Q., Chen, Y., Chen, J., Wang, L., 2011. Modern sedimentation rates and dry-humid change inferred from grain size records in Dianchi Lake, Yunnan Province. *Journal of Geographical Research* **30**, 161–171.

Wang, Y., Yang, H., Zhang, J., Xu, M., Wu, C., 2015. Biomarker and stable carbon isotopic signatures for 100–200 year sediment record in the Chaihe catchment in southwest China. *Science of the Total Environment* **502**, 266–275.

Whitney, B.S., Mayle, F. E., 2012. *Pediastrum* species as potential indicators of lake-level change in tropical South America. *Journal of Paleolimnology* **47**, 601–615.

Wu, D., Zhou, A., Chen, X., Yu, J., Zhang, J., Sun, H., 2015a. Hydrological and ecosystem response to abrupt changes in the Indian monsoon during the last glacial, as recorded by sediments from Xingyun Lake, Yunnan, China. *Palaeogeography, Palaeoclimatology, Palaeoecology* **421**, 15–23.

Wu, J., Zhang, Q., Li, A., Liang, C., 2015b. Historical landscape dynamics of Inner Mongolia: patterns, drivers, and impacts. *Landscape Ecology* **30**, 1579–1598.

Xi, Y.Z., Ning, J.C., 1994. Study on pollen morphology of plants from dry and semidry area in China. *Yushania* **11**, 119–191.

Xiao, J., Chang, Z., Si, B., Qin, X., Itoh, S., Lomtatidze, Z., 2009. Partitioning of the grain-size components of Dali Lake core sediments: evidence for lake-level changes during the Holocene. *Journal of Paleolimnology* **42**, 249–260.

Xiao, J., Fan, J., Zhou, L., Zhai, D., Wen, R., Qin, X., 2013. A model for linking grain-size component to lake level status of a modern clastic lake. *Journal of Asian Earth Sciences* **69**, 149–158.

Xiao, X., Yao, A., Hillman, A., Shen, J., Haberle, S.G., 2020. Vegetation, climate and human impact since 20 ka in central Yunnan Province based on high-resolution pollen and charcoal records from Dianchi, southwestern China. *Quaternary Science Reviews* **236**, 106297. https://doi.org/10.1016/j.quascirev.2020.106297.

Yang, X., Yang, C., Meng, Z., 2016. The current situation, problems and suggestions of grassland ecological protection in China. *Pratacultural Science* **33**, 1901–1909.

Yin, H., Pflugmacher, D., Li, A., Li, Z., Hostert, P., 2018. Land use and land cover change in Inner Mongolia—understanding the effects of China's re-vegetation programs. *Remote Sensing of Environment* **204**, 918–930.

Zhang, G., Yao, T., Piao, S., Bolch, T., Xie, H., Chen, D., Gao, Y., *et al.*, 2017. Extensive and drastically different alpine lake changes on Asia's high plateaus during the past four decades. *Geophysical Research Letters* **44**, 252–260.

Zhang, J., Jin, M., Chen, F., Battarbee, R.W., Henderson, A.C.G., 2003. High-resolution precipitation variations in the northeast Tibetan Plateau over the last 800 years documented by sediment cores of Qinghai Lake. *Chinese Science Bulletin* **48**, 1451–1456.

Zhang, X., Xu, B., Li, J., Xie, Y., Gleixner, G., 2021. Late-Holocene fluctuations of monsoonal Qiangyong Glacier, southern Tibetan Plateau. *The Holocene* **31**, 1138–1147.

Zhang, Y., Xu, X., Liao, Z., Han, Z., Ji, G., Liang, W., Liu, T., 2021. Response of surface runoff to land use and land cover change and its impact on Daihai Lake shrinkage in Inner Mongolia, China. *Theoretical and Applied Climatology* **144**, 555–569.

Zhang, Z., Shen, Z., Zhang, S., Chen, J., Chen, S., Li, D., Zhang, S., *et al.*, 2023. Lake level evidence for a mid-Holocene East Asian summer monsoon maximum and the impact of an abrupt late-Holocene drought event on prehistoric cultures in north-central China. *The Holocene* **33**, 382–399.

Zhao, Y., Liu, H., Li, F., Huang, X., Sun, J., Zhao, W., Herzschuh, U., Tang, Y., 2012. Application and limitations of the *Artemisia*/Chenopodiaceae pollen ratio in arid and semi-arid China. *The Holocene* **22**, 1385–1392.

Zhao, Y., Yu, Z., Chen, F., Ito, E., Zhao, C., 2007. Holocene vegetation and climate history at Hurleg Lake in the Qaidam Basin, northwest China. *Review of Palaeobotany and Palynology* **145**, 275–288.

Zhen, Z., Li, W., Xu, L., Zhang, X., Zhang, J., 2021. Lake-level variation of Dali Lake in mid-east of inner Mongolia since the Late Holocene. *Quaternary International* **583**, 62–69.